Very Long Baseline Interferometry and the VLBA
ASP Conference Series, Vol. 82, 1995
J. A. Zensus, P. J. Diamond, and P. J. Napier (eds.)

Printed June 13, 1995

CHAPTER 21

VLBI Observing Strategies

J. M. WROBEL
NATIONAL RADIO ASTRONOMY OBSERVATORY

Abstract A step-by-step guide to planning a VLBI imaging project is presented, with emphasis on practical aspects.

Contents

21.1 Select a Target

Pick a nifty astronomical target to image, and assess whether or not it is a sensible VLBI target. Two issues are especially important. First, what is the target's flux density S in units of Janskys? S is needed for realistic signal-to-noise ratio calculations to be done in section 21.7.3. It is best if S is from a previous VLBI detection, since S then refers to milli arcsecond (mas) scales. It is acceptable if S is from a connected-element array like the VLA or WSRT, as such arrays probe arcsecond scales. It is poor practice to adopt S from a single dish because such a flux density typically encompasses arcminute scale structure. Second, is there evidence for mas-scale structure in the target? Knowledge of a prior VLBI detection is best. However, it is acceptable if the target is known to be unresolved with a connected-element array. Another good indicator of mas-scale structure is flux density variability, since only physically small sources can vary on time scales of hours to years. This presents a complication, though, since it means a recent $S(t)$ or a typical S is needed for making realistic signal-to-noise calculations. An emission line target known to be masing generally will exhibit mas-scale structure. A synchrotron continuum target with a flat radio spectrum is usually synchrotron-self-absorbed, implying it will probably possess mas-scale structure. If the target is a sensible one for VLBI, then proceed.

For a line target, whether observed in emission or absorption, the transition rest frequency $\nu_{\rm R}$ is needed to ascertain if potential VLBI arrays have an appropriate receiver. Various VLBI documents discuss receiver availability (Alef and Mantovani 1995; Wrobel 1994; Wrobel and Claussen 1994). Generally, most major atomic and molecular absorption lines are doable (e.g., HI, H_2CO), as are most major maser emission lines (e.g., OH, H_2O). However, the 6 GHz methanol maser is usually missed. If an appropriate receiver is available for the desired transition, then assemble a few other facts concerning the line target. First, what is the relative earth-target motion along the line-of-sight? This is needed to make the Doppler transformation required to ascertain the exact observing frequency $\nu_{\rm O}$ required. Usually this relative radial motion is expressed in terms of a velocity relative to the local standard of rest $v_{\rm LSR}$ or a velocity relative to that of the Sun $v_{\rm HELIO}$. Roelfsema (1989) discusses these and other velocity rest frames. van Gorkom et al. (1989) is highly recommended reading for extragalactic line observers forced to grapple with redshift definitions and their relations to radial velocities. Second, what is the spread of lines ΔV? This is needed to help define the desired recorded bandwidth $\Delta\nu_{\rm REC}$, discussed in section 21.6. Third, what are the widths of individual lines Δv? These line widths are required to select an appropriate frequency resolution.

21.2 Desired Angular Resolution

The desired angular resolution $\theta_{\rm HPBW}$ is set by the astronomical goals of the VLBI project. To give a concrete example that will be returned to often in this lecture, consider the radio continuum nucleus of the Seyfert 1 galaxy NGC 5548. Three nuclear traits inferred from VLA data suggest mas-scale structure: an angular size < 200 mas; a time-variable flux density with a typical $S_{8.4\ \rm GHz} \sim$ 2 mJy; and a flat radio spectrum. The scientific issue to be addressed with VLBI is the mas radio morphology. Does it show a standard core-jet morphology, indicative of being driven by a central monster, possibly a supermassive black hole? Or, does it conform to the starburst theory predictions of one or two radio supernovae or compact supernova remnants, each smaller than 1 mas in diameter and confined to a starburst disk 20 mas in diameter? For this project,

$\theta_{\rm HPBW} \sim 1$ mas is an appropriate choice.

When selecting $\theta_{\rm HPBW}$, it is important to understand that diffuse emission can disappear if $\theta_{\rm HPBW}$ is too small. Consult, for example, the 18 cm VLBI image of the quasar 3C 48 presented as a false-color image in figure 1 of Wilkinson et al. (1991). (This is a superb VLBI image, and your life will not be complete unless you see it!). This image has $\theta_{\rm HPBW} \sim 6$ mas and a root-mean-square (rms) image noise $\Delta I_{\rm m} \sim 1/2$ mJy beam^{-1}, plus extensive diffuse regions with surface brightnesses as low as $I_{\rm m} \sim 2$ mJy beam^{-1} color coded as purple. Suppose a hypothetical VLBI project yielded a new image of 3C 48 with similar noise characteristics but with $\theta_{\rm HPBW} \sim 1$ mas. Then regions in the old image at ~ 2 mJy beam^{-1} would, in the new image, be diminished in brightness by the ratio of the new to the old synthesized beam areas. The new brightness would be only $\sim 1/18$ mJy beam^{-1}, well below the rms image noise: thus these diffuse regions would disappear!

21.3 Desired Largest Angular Scale

What is the largest angular scale $\theta_{\rm LAS}$ you want to image? $\theta_{\rm LAS}$ is generally fixed, or at least constrained, by a prior VLBI detection, by a size limit from a connected-element array, and/or by theory. If uncertain about a value for $\theta_{\rm LAS}$, try for $\sim$ 10–20 $\times\ \theta_{\rm HPBW}$ to ensure that a reasonable range of angular scales will be probed. For the NGC 5548 example, this reasoning suggests $\theta_{\rm LAS} \sim$ 10–20 mas. Don't confuse $\theta_{\rm LAS}$ with the separation of point-like sources: if NGC 5548 contains two unresolved radio supernovae separated by $\theta_{\rm SEP}$, then $\theta_{\rm SEP} \neq \theta_{\rm LAS}$. As will be discussed in section 21.7.5, $\theta_{\rm SEP}$ is related to the undistorted field of view offered by the VLBI array.

21.4 Desired Observing Frequency

Most line projects offer little or no flexibility regarding the desired observing frequency $\nu_{\rm O}$. The physics dictates the transition rest frequency $\nu_{\rm R}$, and Doppler corrections for the relative earth-target radial motions yield an exact observing frequency $\nu_{\rm O}$. As a Galactic example, consider the methanol maser emission from the Orion K-L object with $v_{\rm LSR} = 9.0$ km s^{-1}. Methanol transition A has $\nu_{\rm R} = 25.01812$ GHz, so $\nu_{\rm O}$ can (just) be reached with a 1.3 cm receiver. Methanol transition B has $\nu_{\rm R} = 44.06943$ GHz, requiring 7 mm observations. Since it is usually easier to work at 1.3 cm than at 7 mm, probing the methanol emission from this target offers some frequency flexibility *as long as the astronomical goals are not compromised.* If the scientific issue to be addressed is the pumping mechanism for the 7 mm maser, then there is no choice: the more technically difficult 7 mm observations would be required.

As an extragalactic example, consider the flat-spectrum radio continuum source 4C 31.04, against which the VLA and Arecibo detect HI in absorption, with a line spread $\Delta V \sim 160$ km s^{-1} and at a velocity close to the optical heliocentric recession velocity $v_{\rm HELIO} \sim 17391$ km s^{-1} of the host elliptical galaxy (van Gorkom et al. 1989; Mirabel 1990). VLBI continuum imaging shows a double source at 90 cm, with an eastern and a western component separated by a few tens of milliarcseconds (Wrobel and Simon 1986). If, as seems plausible, the 20 cm continuum shows a similar morphology, then an interesting scientific issue is: In a VLBI image, is the HI "seen" in absorption against the eastern component, the western component, or both components? The observing frequency required for the HI VLBI project is $\nu_{\rm O} = \nu_{\rm R}/(1 + z_{\rm HI}) = 1341$ MHz, where $z_{\rm HI}$ is the redshift of the HI absorption as measured by the VLA or Arecibo, and $\nu_{\rm R} = 1420.4$ MHz is the well-known HI rest frequency. Clearly, such a project has no frequency flexibility at all. It is thus important to ensure that a potential VLBI array can tune to 1341 MHz (cf. section 21.7.1). In principle, the answer is probably yes; but in practice, redshifted HI observers must be aware that radio frequency interference (RFI) local to the antennas comprising the VLBI array can degrade the performance of the array.

Most VLBI projects involving continuum targets have reasonable frequency flexibility. For example, VLA data indicate that the NGC 5548 nucleus has $S_{5\ \rm GHz} \sim S_{8.4\ \rm GHz} \sim 2$ mJy. Thus the frequency selection can be made based on the expected VLBI array performance. As will be argued below, the VLA should be included as an element of the VLBI array, and since the VLA currently is much more sensitive at 8.4 GHz than at 5 GHz, the higher frequency is obviously preferred.

Some projects, whether involving line or continuum targets, need multiple frequencies from a single receiver; i.e., they span moderate bandwidths $\Delta\nu_{\rm SPAN}$. Examples are multi-frequency synthesis (see chapter 16) and Faraday-effect projects. One of two methods can be applied to acquire multiple frequencies from a single receiver:

1. *Single-Receiver Method S1:* Split the desired recorded bandwidth $\Delta\nu_{\rm REC}$, discussed in section 21.6, up among the desired frequencies and observe at those fixed frequencies. A disadvantage of this method is that only part of the full recorded bandwidth applies to each of the fixed frequencies, resulting in higher noise levels; while an advantage is that similar (u, v) plane coverages are obtained for each fixed frequency.

2. *Single-Receiver Method S2:* Get the full desired $\Delta\nu_{\rm REC}$ at each frequency by cycling scans among the frequencies as the observations progress. A disadvantage of this method is that dissimilar (u, v) plane coverages are obtained for each frequency. This method requires "frequency agility" for each antenna in the VLBI array, i.e. quick computer-selection of different frequencies.

Some projects, such as those involving scatter-broadened targets, need multiple frequencies from two or more receivers. There are three methods of obtaining such multiple frequencies:

1. *Multiple-Receivers Method M1:* Access two or more receivers simultaneously during a single track in the (u, v) plane. An advantage is that the same, possibly full, (u, v) plane coverage can be obtained with each receiver; while a disadvantage is the reduced $\Delta\nu_{\mathrm{REC}}$ per receiver. Simultaneous dual frequency observations are often done using the 13/4 cm receiver pair commonly available on many VLBI antennas.

2. *Multiple-Receivers Method M2:* Access two or more receivers sequentially during a single track in the (u, v) plane. A disadvantage is the reduced (u, v) plane coverage per receiver, leading to a poorer "dirty beam". An advantage is that the full $\Delta\nu_{\mathrm{REC}}$ is obtained for each receiver. This observing method requires "receiver agility", i.e. quick computer-selection of different receivers. Receiver-agile VLBI arrays are particularly invaluable tools for monitoring the structural evolution of transient phenomena like radio supernovae.

3. *Multiple-Receivers Method M3:* Access two or more receivers contemporaneously, with each receiver available only during a single track in the (u, v) plane. Advantages are that the same, possibly full, (u, v) plane coverage can be obtained with each receiver, plus the full $\Delta\nu_{\mathrm{REC}}$ is available for each receiver. For example, during a typical VLBI Network session three (u, v) plane tracks can be obtained within a time span of three weeks using 1.3 cm, 6 cm, and 18 cm receivers. A concern about this observing style is that the VLBI target may have experienced strength and/or structural variations between the separate (u, v) plane tracks, which could complicate analysis of the multi-frequency data.

Some projects, whether involving line or continuum targets, need matched θ_{HPBW} at multiple frequencies. Examples include spectral index and Faraday effect projects. If it is adequate to have the multiple frequencies come from a single receiver, then the resultant VLBI images can just be restored with the worst θ_{HPBW}, generally that from the lowest observing frequency. However, if the multiple frequencies must come from two or more receivers, then this can be much more challenging to arrange. In the case of the VLA, an appropriate set of frequencies is selected and each frequency is observed with an appropriate VLA configuration; or an appropriate VLA subarray; or, if the frequencies are not too different, with the same VLA configuration but with appropriate (u, v) plane weighting schemes employed during image formation. In the VLBI case, an appropriate set of frequencies is selected and each is observed either with different VLBI arrays, or with the same arrays but with application of appropriate (u, v) plane weighting functions during image formation. In the past, VLBI subarraying by frequency was rarely done, due to the small number of antennas available and the general lack of receiver agility. However, this observing style may well become more popular: with the advent of the VLBA correlator, projects involving up to 20 antennas are now feasible, and a growing subset of those 20 are fully receiver agile, permitting easy subarraying by frequency.

21.5 Desired Stokes Parameters

Linear polarimetrists require RR, LL, RL, and LR correlations. From them, they form Stokes parameters I, Q, and U, which in turn yield the linear polarization flux density $P = \sqrt{Q^2 + U^2}$, the linear polarization percentage $m_{\rm L} = P/I$, and the linear polarization position angle $\chi = \frac{1}{2}\arctan U/Q$. Circular polarimetrists need RR and LL correlations, from which are formed Stokes parameters I and V, which are then combined to give the circular polarization percentage $m_{\rm c} = V/I$. Simple detection projects should probably be done in either RR or LL, to avoid needing to do a RR-LL phase alignment. For example, RR alone is fine for the NGC 5548 project. However, both *RR and LL* could be needed for *very* sensitive detection projects, as such projects no doubt involve the phased VLA and/or Arecibo, instruments that currently can provide only a few tens of MHz bandwidth per polarization.

21.6 Desired Recorded Bandwidth

The desired recorded bandwidth $\Delta\nu_{\rm REC}$ is intricately linked to the recording formats available, the bits per sample available, the possibility of oversampling at OS time the Nyquist rate, and the consequent aggregate bit rate, defined as $ABR = 2 \times \Delta\nu_{\rm REC} \times OS \times \frac{\rm bits}{\rm sample}$. For VLBI line targets, there is a natural limit to $\Delta\nu_{\rm REC}$. If the spread of the lines is ΔV, then the corresponding frequency spread can be approximated with $\Delta\nu_{\rm LINE}/\nu_{\rm O} = \Delta V/c$. Add a bit of extra padding to $\Delta\nu_{\rm LINE}$, to allow the continuum or zero level to be "seen" and to ensure an approximately flat pass band in the spectral region of interest. This sets the desired recorded bandwidth $\Delta\nu_{\rm REC}$. For the extragalactic HI absorption example from section 21.4, $\Delta\nu_{\rm LINE} = 716$ kHz, suggesting selection of $\Delta\nu_{\rm REC} = 2$ MHz. For VLBI continuum targets, there is no natural limit to $\Delta\nu_{\rm REC}$. However, there are practical limits due to ABR limits discussed below, due to bandwidth smearing discussed in section 21.7.5, and due to bandwidth depolarization (Rudnick, Zukowski and Kronberg 1983).

At sites with VLBA backends, baseband signals to be used in VLBA format recordings are derived from up to eight baseband converters (BBCs). Each BBC provides one or two signals, one arising from an upper sideband (USB) mix and one from a lower sideband (LSB) mix. A baseband (BB) channel is defined as coming from a single sideband associated with a BBC. Thus, the VLBA provides up to 16 BB channels. The bandwidth per BB channel $\Delta\nu_{\rm BB}$ ranges up to 16 MHz. The recorded bandwidth $\Delta\nu_{\rm REC}$ is just the sum of the bandwidths from each of up to 16 activated BB channels. The BB channel signals can be encoded as 1- or 2-bit samples, and it is also possible to oversample relative to the Nyquist rate. Projects involving line targets generally do not require high

*ABR*s, so such projects should certainly be done with 2-bit samples and should possibly be done with oversampling. Projects involving continuum targets will generally be *ABR* limited, for the following reason: operational considerations impose a "sustainable" *ABR* limit of 128 million bits per second (Mbps), thus effectively imposing a $\Delta\nu_{\rm REC}$ limit. For example, the VLBA format continuum mode selected for NGC 5548 is called "128-4-2-R", meaning an $ABR = 128$ Mbps, four BB channels, two bits per sample, and RCP only. This results in $\Delta\nu_{\rm REC} = 32$ MHz, with $\Delta\nu_{\rm BB} = 8$ MHz coming from each BB channel. The VLBA can also record some Mark III formats.

At sites with Mark III backends, baseband signals to be used in Mark III format recordings are derived from 14 video converters (VCs), with one or two sidebands (USB, LSB) from each VC. Thus there are 28 possible BB channels. The bandwidth per BB channel $\Delta\nu_{\rm BB}$ ranges up to 4 MHz. The recorded bandwidth $\Delta\nu_{\rm REC}$ is just the sum of the bandwidths from each of up to 28 activated BB channels. The BB channel signals can be encoded only as 1-bit samples, meaning $ABR = 2 \times \Delta\nu_{\rm REC} \times 1$. As a continuum example involving Mark III format recordings, consider NGC 5548. A possible Mark III format continuum mode at 4 cm is called "B", meaning an *ABR* of 56 Mbps, fourteen BB channels, one bit per sample, and RCP only. This results in $\Delta\nu_{\rm REC} = 28$ MHz, with $\Delta\nu_{\rm BB} = 2$ MHz coming from each BB channel. Rogers et al. (1983) and Alef (1989b) provide many more Mark III details. Efforts to upgrade the Mark III system to its next evolutionary step, called Mark IV, are currently underway at Haystack Observatory (see chapter 6). Mark IV has an *ABR* target of 1 Gbps. Mark IV format recordings will be more compatible with VLBA format recordings, mainly by providing wider BB channel bandwidths.

A single sideband from a Mark III VC or a VLBA BBC can be recorded in Mark II format (Clark 1973). The recorded bandwidth is 2 MHz or less. Only 1-bit samples and a fixed *ABR* of 4 Mbps are possible. Note, however, that the ability to correlate such projects is disappearing rapidly: all Mark II correlators are closed down for *in absentia* correlation. Proposers of Mark II format projects must thus make arrangements, prior to their observations, for special access to correlation facilities.

21.7 Select and Evaluate a Trial VLBI Array

Consult various VLBI documentation for the information needed to select antennas for a trial VLBI array. For example, *The European VLBI Network Handbook* (Alef and Mantovani 1995) is a very useful resource for those planning projects involving European VLBI Network (EVN) antennas. The *VLBA Observational Status Summary* (Wrobel 1994) currently fills a similar role for the VLBA, while *Very Long Baseline Interferometry at the Very Large Array* (Wrobel and Claussen 1994) should be consulted if inclusion of the VLA is contemplated. Having selected a trial VLBI array, sections 21.7.1 through 21.7.5 below describe how to evaluate various key properties of the trial array. It will be assumed that just a single receiver or two simultaneous receivers are needed. If this is not true, then a new trial array might have to be selected and evaluated for each receiver required.

21.7.1 Special Needs Evaluation

Do the antennas in the trial array meet the project's special needs, if any? For example, dual polarization receivers will be needed for linear polarization projects. Similarly, projects involving multi-frequency synthesis, extragalactic line targets, and Faraday effect studies could be difficult at certain antennas because of restricted receiver tuning ranges. Adjust the antennas selected for the trial array if necessary. Otherwise end the special needs assessment and proceed to the geometry assessment.

21.7.2 Geometric Evaluation

Acquire the software tools needed to assess the geometry of the trial array. In particular, when is the target "visible" to antennas in the array? What range of angular scales are probed? How well is the (u, v) plane sampled, whether in a full track or in multiple snapshots? The multiple-snapshot style could be due to many different targets being observed with a fixed receiver or simultaneous receiver pair; or due to one target being observed with a receiver-agile VLBI array asked to cycle among receivers. Software tools for geometric evaluation can be found in the Caltech VLBI analysis programs (Pearson 1991); in Haystack Observatory's PC-SCHED program; and (eventually) in NRAO's VLBA OBSERVE program.

Even without such tools, one can easily determine if the trial array provides the desired $\theta_{\rm HPBW}$ and $\theta_{\rm LAS}$, discussed in section 21.2 and section 21.3, respectively. Knowing the observing wavelength in cm $\lambda_{\rm O}^{\rm cm}$ (section 21.4), plus the minimum baseline in km $B_{\rm min}^{\rm km}$ and the maximum baseline in km $B_{\rm max}^{\rm km}$ offered by an array, the following formulae can be used to evaluate $\theta_{\rm HPBW}$ in mas and $\theta_{\rm LAS}$ in mas:

$$\theta_{\rm HPBW}^{\rm mas} \sim 2063 \times \lambda_{\rm O}^{\rm cm} / B_{\rm max}^{\rm km} \tag{21.1}$$

$$\theta_{\rm LAS}^{\rm mas} \sim 2063 \times \lambda_{\rm O}^{\rm cm} / (2 \times B_{\rm min}^{\rm km})\,. \tag{21.2}$$

Twice $B_{\rm min}^{\rm km}$ is used in equation 21.2 to ensure that a good job is done on $\theta_{\rm LAS}$. Application of these equations to the VLBA are shown in figure 21.1. If the values for $\theta_{\rm HPBW}^{\rm mas}$ and $\theta_{\rm LAS}^{\rm mas}$ are inappropriate, then adjust the antennas selected for the trial array. Otherwise, continue.

Another issue related to the geometry of the trial VLBI array is whether or not it has "enough" antennas. With N antennas, how many synthesized beam areas $\Omega_{\rm b}$, approximated as $\Omega_{\rm b} = 1.13 \times \theta_{\rm HPBW}^2$, can be well reconstructed in an extended target of angular area $\Omega_{\rm t}$? Readhead and Wilkinson (1978) argue that,

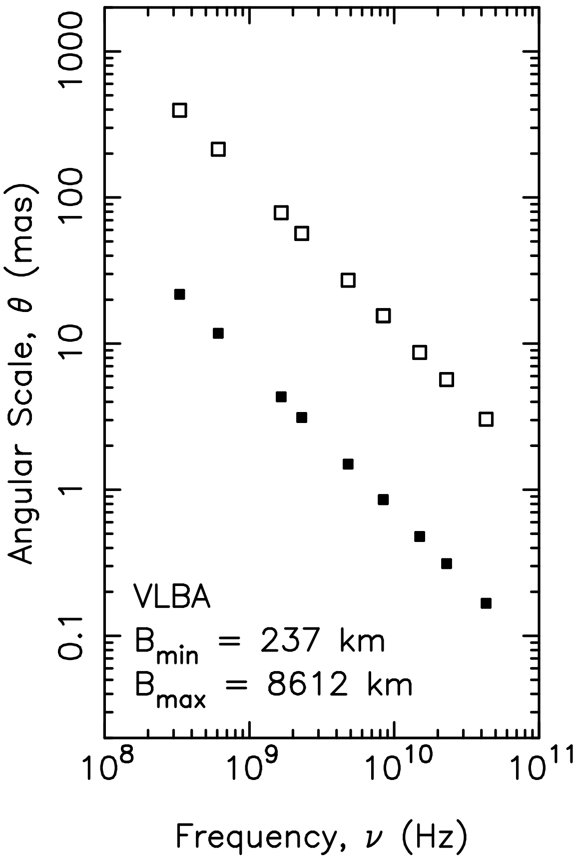

Figure 21.1: Equation 21.1 *(closed symbols)* and equation 21.2 *(open symbols)*, both for the VLBA.

for roughly uniform (u, v) plane coverage:

$$\frac{\Omega_{\mathrm{t}}}{\Omega_{\mathrm{b}}} \lesssim \left(\frac{N \times (N-1)}{2}\right)^2 . \tag{21.3}$$

This is clearly a less limiting constraint for a one-dimensional target than it is for a two-dimensional target. Adjust the antenna selection if necessary. Otherwise, end the geometry assessment of the trial array and continue to the baseline sensitivity assessment.

21.7.3 Baseline Sensitivity Evaluation

The rms thermal noise during the fringe-fit interval in the real or imaginary component of the visibility of either the RR or the LL baseline between antennas

i and j is (see chapter 8, and Walker (1989c)):

$$\Delta S_{\mathrm{ij}} = \frac{1}{\eta_{\mathrm{s}}} \times \sqrt{\frac{SEFD_{\mathrm{i}} \times SEFD_{\mathrm{j}}}{2 \times \Delta\nu \times \tau_{\mathrm{ff}}}} . \tag{21.4}$$

Comments on the terms in equation 21.4 follow:

1. $\eta_{\mathrm{s}} \leq 1$: This accounts for the VLBI system inefficiency. Adopt $\frac{1}{\eta_{\mathrm{s}}} \sim 2$ for 1-bit samples. About the same noise results from 2-bit samples and half the bandwidth.

2. $SEFD_{\mathrm{i}}$ and $SEFD_{\mathrm{j}}$ are the system equivalent flux densities of antennas i and j in units of Janskys.

3. $\Delta\nu$ is the bandwidth in units of Hz. Use $\Delta\nu_{\mathrm{REC}}$ for a continuum target (see section 21.6). However, for a line target use the width of a spectral channel, which is the BBC or VC bandwidth divided by the number of spectral points SP. For either type of target, information will be needed regarding the various recording schemes, discussed in section 21.6, that are available at the antennas in trial array.

4. τ_{ff} is the fringe-fit interval in units of seconds. Suppose that the antennas to be used all have Hydrogen masers as frequency and time standards. Then at observing frequencies above about 1 GHz, the fringe-fit interval is bounded from above by the atmospheric coherence time τ_{coh} set mainly by tropospheric conditions. Typical values of τ_{coh} to expect are about 16 seconds at 100 GHz, about 160 seconds at 10 GHz, and about 1600 seconds at 1 GHz (Moran 1989). Below about 1 GHz, τ_{coh} can range from a few tens of seconds to a few minutes, depending on conditions in the interplanetary medium and the earth's ionosphere (Simon et al. 1990). Finally, τ_{coh} can be considerably shortened at any frequency if antennas lacking Hydrogen masers are used.

Evaluate equation 21.4 for the baselines in the trial array and then use S from section 21.1 to form realistic signal-to-noise ratios (SNRs) $S/\Delta S_{\mathrm{ij}}$ for these baselines. If these SNRs are less than or the order of a few on the baselines in the trial array, as is true for the NGC 5548 example, then try one or more of the following options:

1. Adjust the parameters in equation 21.4 to lower ΔS_{ij}.

2. Add bigger antennas to the trial array. In the NGC 5548 example, the phased VLA was added.

3. Plan to global fringe-fit. See chapter 10; Rogers (1991); Cotton and Schwab (1993); Rogers (1993b); Rogers (1993c); Kogan (1994); and Rogers, Doeleman and Moran (1995).

4. Plan to phase reference (see chapter 17). This was selected for the NGC 5548 example.

If the SNRs are greater than or the order of a few on the baselines in the trial array, then the source is strong enough for fringe-fitting and subsequent self-calibration.

Linear polarization projects need both parallel (RR, LL) and crossed (RL, LR) hand correlations. However, the fringe-fitting of such data is done using the strong parallel-hand correlations, rather than the weak crossed-hand correlations. Thus the SNR discussions above concerning the parallel hands also apply to linear polarization projects.

Phase referencing must be employed for any target, weak or strong, if absolute α and δ axes are needed either for a single-epoch image or for comparison of images at multiple epochs. The latter need applies to the weak-target example NGC 5548: if it could be shown that old radio supernovae or compact supernova remnants faded between epochs, while new ones appeared at *different* α's and δ's within the nuclear regions, then a starburst origin for the radio emission could be cleanly proven.

21.7.4 Image Sensitivity Evaluation

The rms thermal noise during the on-target integration time in an image made from all RR or all LL baselines among N identical antennas is (Crane and Napier 1989):

$$\Delta I_{\rm m} = \frac{1}{\eta_{\rm s}} \times \frac{SEFD}{\sqrt{N \times (N-1) \times \Delta\nu \times t_{\rm int}}} \, . \tag{21.5}$$

In equation 21.5, $\eta_{\rm s}$, $SEFD$, and $\Delta\nu$ are as defined for equation 21.4, and have the same units as in that equation. $t_{\rm int}$ is the on-source integration time in units of seconds. It will be the order of hours for a full track in the (u, v) plane but could be much less if multiple snapshots are planned. $\Delta I_{\rm m}$ will have units of Jy beam^{-1}. Walker (chapter 8) and Walker (1989c) give the more general expression for an array of non-identical antennas. Either equation 21.5 or the more general expression, whichever is most appropriate, can be used to evaluate $\Delta I_{\rm m}$ for the trial VLBI array. There are, however, two caveats concerning use of these $\Delta I_{\rm m}$ expressions to estimate image noise levels. First, the actual on-source rms noise for a point-like target in an amplitude and phase self-calibrated image will be a factor of $\sqrt{(N-1)/(N-3)}$ higher, and could be even higher for more complicated targets (Cornwell 1981). Second, the rms thermal noise might not even be reached due to dynamic range limitations. Keeping these caveats in mind, ask if $\Delta I_{\rm m}$ is adequately low for your target. If it is not, then try to adjust the parameters involved in $\Delta I_{\rm m}$. If it is adequately low, then continue.

If simultaneous dual polarization data with $\Delta I_{\rm m}$ per polarization are available, then the thermal noise in an image of a Stokes parameter I, Q, U, or V

will obey *gaussian statistics* characterized by a zero mean and an rms noise $\Delta I = \Delta Q = \Delta U = \Delta V = \frac{\Delta I_{\rm m}}{\sqrt{2}}$. Ask if this is adequately low for your project. If it is not, then try adjusting the $\Delta I_{\rm m}$ parameters; if it is, then continue. The thermal noise in an image of the linear polarization flux density P will obey *Rayleigh statistics* characterized by a nonzero mean and an rms noise $\Delta P = 0.655 \times \Delta Q = 0.655 \times \Delta U$ (Wardle and Kronberg 1974; page 261 of Thompson, Moran and Swenson 1986). Again, ask if this is adequately low for your purposes. Either try to adjust the $\Delta I_{\rm m}$ parameters or else continue, depending on the answer.

Realistic image simulations, such as those possible with the Caltech VLBI analysis programs (Pearson 1991), can also greatly assist with image sensitivity evaluation.

21.7.5 Field-of-View Evaluation

A final aspect of trial VLBI array evaluation is to determine if the VLBI target will fit into the array's undistorted field of view (FOV) which spans $\pm\theta_{\rm max}$. Topics impacting the undistorted FOV include time-average smearing, bandwidth smearing, and non-coplanar baselines, plus the angular response functions of the connected-element arrays and the single dishes in the trial VLBI array. Each of these will be quantified below, under the simplifying assumption that the delay tracking center is identical to the phase reference position, which in turn is the same as the pointing position for the VLBI array.

Consider the effects of averaging the fringe-fitted data for a time $\tau_{\rm avg}$. This averaging time will be greater than the correlator accumulation time $\tau_{\rm acc}$ but less than the coherence time $\tau_{\rm coh}$ (see section 21.7.3). A benefit of a long $\tau_{\rm avg}$ is to reduce the data volume, thereby speeding up post-processing efforts. If the data will be self-calibrated, aim for a $\tau_{\rm avg}$ less than or the order of the self-calibration solution interval and keep in mind that a short solution interval is good, as it permits following rapid phase fluctuations. A further advantage of a short $\tau_{\rm avg}$ is that it permits a wider FOV undistorted by time-average smearing. This smearing is approximately azimuthal in the image plane, causing a drop in the response to a point source. If a 10% drop is considered tolerable (but self-calers beware!) then $\theta_{\rm max}$ due to time-average smearing can be derived from equation 6.71 of Thompson, Moran and Swenson (1986) (see also Bridle and Schwab 1989). For an averaging time in minutes $\tau^{\rm m}_{\rm avg}$, $\theta_{\rm max}$ is:

$$\theta_{\rm max} \sim 150 \times \frac{\theta_{\rm HPBW}}{\tau^{\rm m}_{\rm avg}} . \tag{21.6}$$

Consider next the effects of bandwidth averaging the fringe-fitted data. Even for a continuum VLBI project, a VLBI correlator will deliver a coarse spectral line data set with SP spectral points at one or more "AIPS IFs". After throwing out bad end points and performing a bandpass calibration, it is feasible to average over the remaining SPs, for each IF. Doing a subsequent average over the multiple IFs is also possible. Both types of bandwidth averaging will reduce the data volume and thus speed up post-processing efforts. However, it may be desirable to avoid the *SP* and/or IF averaging, for two reasons: to permit separate self-calibration adjustments on individual *SP*s or IFs; and to allow a wider FOV undistorted by bandwidth smearing. This smearing is approximately radial in the image plane, resulting in a drop in the point-source response. If a 10% drop is considered acceptable (again, self-calers beware!) then $\theta_{\rm max}$ set by averaging to a bandwidth $\Delta\nu$ can be derived from equation 6.64 of Thompson, Moran and Swenson (1986) (see also Bridle and Schwab (1989)). For $\Delta\nu$ expressed in the same units as the observing frequency $\nu_{\rm O}$, $\theta_{\rm max}$ is:

$$\theta_{\rm max} \sim 0.8 \times \theta_{\rm HPBW} \times \frac{\nu_{\rm O}}{\Delta\nu}\,. \tag{21.7}$$

Non-coplanar baselines in a trial VLBI array can also limit the undistorted FOV. If phase errors of 0.1 radians are deemed acceptable, then the consequent $\theta_{\rm max}$ limitation follows from equation 4.7 of Thompson, Moran and Swenson (1986) (see also Perley 1989). For a maximum baseline in cm $B^{\rm cm}_{\rm max}$ and an observing wavelength in cm $\lambda^{\rm cm}_{\rm O}$, $\theta_{\rm max}$ is:

$$\theta_{\rm max} \sim \frac{\theta_{\rm HPBW}}{3} \times \sqrt{\frac{B^{\rm cm}_{\rm max}}{\lambda^{\rm cm}_{\rm O}}}\,. \tag{21.8}$$

A connected-element array can be "tied" or "phased" to perform as a single element in the trial VLBI array. If such a phased array provides an instantaneous, naturally-weighted synthesized beam at FWHM $\theta_{\rm CE}$, then the corresponding limitation imposed on $\theta_{\rm max}$ is:

$$\theta_{\rm max} \sim \frac{1}{2} \times \theta_{\rm CE}\,. \tag{21.9}$$

An important FOV aspect of phased array use is that weak, mJy-level VLBI targets that must be observed in "extended phasing" mode require a priori positions accurate to a fraction of the synthesized beamwidth. This can correspond to only a few tens of mas for the VLA, depending on its configuration and the observing frequency (Wrobel and Claussen 1994).

FOV limitations are also imposed by the primary beams of the single dishes in the trial VLBI array. For a dish diameter in cm $D^{\rm cm}$ and an observing wavelength in cm $\lambda^{\rm cm}_{\rm O}$, the consequent $\theta_{\rm max}$ limit is:

$$\theta_{\rm max} \sim \frac{1}{2} \times \frac{\lambda^{\rm cm}_{\rm O}}{D^{\rm cm}}\,. \tag{21.10}$$

In practice, such limits are rarely important for VLBI projects. However, when an antenna's pointing is poor in comparison with its primary beamwidth, then the antenna's *SEFD* can be raised above its nominal level.

If evaluation of the various limiting $\theta_{\max}$'s of the trial VLBI array indicates that the VLBI target extends beyond $\pm\theta_{\max}$, then try to adjust the "offending" parameters. Otherwise, this ends the assessment of the trial array's undistorted FOV, which in turn marks the end of the entire trial VLBI array assessment. The trial VLBI array now becomes the desired VLBI array.

21.8 Optimal Times, Seasons, or Years to Observe?

Since VLBI arrays can span many time zones, it may seem silly to try to identify an optimal time-of-day for observing. However, this can be a useful approach for centrally condensed VLBI arrays like the VLBA. For example, nighttime observations offer the benefits of improved antenna pointing, better connected-element array phasing, reduced ionospheric effects, and reduced earth-origin RFI. Earth season effects deserve similar attention. For example, since winter is generally "dry", it is reasonable to attempt to use a VLBI array in local winter to accrue the benefits of a reduced atmospheric opacity and improved connected-element array phasing, while keeping in mind the risk that a few antennas may be experiencing an on-going winter storm and/or have snow in their dishes from recent storms. Finally, Solar cycle effects should also be considered. The earth's ionosphere is most active during Solar maxima, and it is clear that active ionospheric conditions can decrease coherence times at low observing frequencies; they can degrade the calibration of linear polarization position angles, or even make that calibration impossible; and they can degrade the quality of phase-referenced projects done with only a single receiver. It might thus be worthwhile to consider delaying such projects until an upcoming Solar minimum; the next one is expected in about 1997 (NOAA 1993).

21.9 Submit an Observing Proposal

Proposal submission details can be found in the NRAO *Newsletter*, in Wrobel (1994) for the VLBA and its affiliates, and in Alef and Mantovani (1995) for the EVN and its affiliates.

21.10 Make Antenna and Tape Control Schedule Files

Successful proposers must make ASCII schedule files to control the antenna and tape motions in the VLBI array. Users allocated VLBI observing time on the VLBA and/or VLA can consult the general schedule file preparation instructions appearing in Wrobel (1994). In addition, such users will be sent, usually by e-mail, more detailed and up-to-date schedule file preparation instructions.

The schedule files should point the VLBI array at the target, at "strong calibrators", and at "other calibrators". The target must have an a priori position accurate enough for the single dishes and the connected-element arrays in the VLBI array. Modern antennas and correlators prefer J2000 coordinates; if only a B1950 position is available for the target, use any VLBI schedule-making program to convert it to J2000. Strong calibrators are used to find fringes, to estimate actual coherence times, to do bandpass calibration, and to do a "manual" pulse calibration in case the appropriate hardware either fails or is unavailable. A strong calibrator needs an a priori position accurate to a few mas or less at correlation time, to be most useful for fringe-finding purposes. The other calibrators are required to check the a priori amplitude calibration information provided by the staff of the antennas in the VLBI array; to calibrate the instrumental antenna polarizations, if appropriate; to reference the phases, if appropriate; and to calibrate the delays for a line target. A phase calibrator needs an a priori position accurate to a few mas or less at correlation time, to be most useful for phase referencing.

21.11 Correlator Tolerance on Target Positional Errors

After a priori model removal, data from the VLBI correlator must have a residual fringe within a window of full width $1/\tau^{\rm s}_{\rm acc}$, where $\tau^{\rm s}_{\rm acc}$ is the correlator accumulation time in units of seconds. What is the a priori position error $\Delta\theta_{\rm R}$ in arcseconds such that the target *misses* this fringe-rate window? Assume a perfectly known maximum baseline at transit of length $B^{1000\ {\rm km}}_{\rm max}$ in units of 1000 km and an observing wavelength in cm $\lambda^{\rm cm}_{\rm O}$. Then equation 12.20 of Thompson, Moran and Swenson (1986) can be used to estimate $\Delta\theta_{\rm R}$:

$$\Delta\theta_{\rm R} \geq \frac{14\ {\rm arcsec} \times \lambda^{\rm cm}_{\rm O}}{\tau^{\rm s}_{\rm acc} \times B^{1000\ {\rm km}}_{\rm max}}\,. \tag{21.11}$$

In practice, a position much more accurate than $\Delta\theta_{\rm R}$ should be provided before correlation to permit use of a tighter fringe-fit search window, thereby reducing the chance of finding a noise peak and allowing a lower fringe detection threshold to be adopted.

Similarly, after a priori model removal, data from the VLBI correlator must have a residual delay within a window of full width $1/(\frac{\Delta\nu_{\rm BB}}{SP})$, where $\Delta\nu_{\rm BB}$ is the BB channel width in units of Hz and SP is the number of spectral points per BB channel. What is the a priori position error $\Delta\theta_{\rm D}$ in arcseconds such that the target *misses* this delay window? Again assume a perfectly known maximum baseline at transit of length $B^{1000\ {\rm km}}_{\rm max}$ in units of 1000 km. Then letting $\Delta\nu^{\rm MHz}_{\rm BB}$ be the BB channel width in units of MHz, equation 12.19 of Thompson, Moran and Swenson (1986) provides an estimate of $\Delta\theta_{\rm D}$:

$$\Delta\theta_{\rm D} \geq 31\ {\rm arcsec} \times \frac{1}{\frac{\Delta\nu^{\rm MHz}_{\rm BB}}{SP} \times B^{1000\ {\rm km}}_{\rm max}}\,. \tag{21.12}$$

A position much more accurate than $\Delta\theta_{\rm D}$ should be provided prior to correlation, to reap the same benefits as outlined in the $\Delta\theta_{\rm R}$ case.

I thank Craig Walker for substantial comments on the content of this lecture.

References

Alef, W. 1989. "Introduction to phase reference mapping". See Felli and Spencer (1989), p. 261.

Alef, W., & Mantovani, F. 1995. *The European VLBI Network Handbook.* Bologna: Istituto di Radioastronomia.

Bridle, A. H., & Schwab, F. R. 1989. "Wide field imaging I: Bandwidth and time-average smearing". See Perley, Schwab and Bridle (1989), p. 247.

Clark, B. G. 1973. "The NRAO tape-recorder interferometer system". *IEEE Proc.* **61**, 1242.

Cornwell, T. J. 1981. "An error analysis of calibration". VLA Scientific Memorandum 135, National Radio Astronomy Observatory.

Cotton, W. D., & Schwab, F. R. 1993. "Point source detection thresholds for global fringe fitting". VLBA Scientific Memorandum 2, National Radio Astronomy Observatory.

Crane, P. C., & Napier, P. J. 1989. "Sensitivity". See Perley, Schwab and Bridle (1989), p. 139.

Felli, M., & Spencer, R. (Eds.) 1989. *Very Long Baseline Interferometry*, Volume 283 of *NATO ASI Series C.* Dordrecht: Kluwer.

Kogan, L. 1994. "Another approach to estimation of detection threshold for global fringe fitting". VLBA Scientific Memorandum 7, National Radio Astronomy Observatory.

Mirabel, I. F. 1990. "Atomic hydrogen in radio galaxies: A high-velocity cloud moving toward the giant elliptical 4C 31.04". *Astrophys. J.* **352**, L37.

Moran, J. M. 1989. "Introduction to VLBI". See Felli and Spencer (1989), p. 27.

NOAA 1993. *Solar-Geophysical Data Prompt Reports.* Boulder: National Oceanic and Atmospheric Administration. Monthly serial.

Pearson, T. J. 1991. "Caltech VLBI analysis programs". *Bull. Am. Astron. Soc.* **23**, 991.

Perley, R. A. 1989. "Wide-field imaging II: Imaging with non-coplanar arrays". See Perley, Schwab and Bridle (1989), p. 259.

Perley, R. A., Schwab, F. R., & Bridle, A. H. (Eds.) 1989. *Synthesis Imaging in Radio Astronomy.* San Francisco: Astronomical Society of the Pacific.

Readhead, A. C. S., & Wilkinson, P. N. 1978. "The mapping of compact radio sources from VLBI data". *Astrophys. J.* **223**, 25.

Roelfsema, P. 1989. "Spectral line imaging I: Introduction". See Perley, Schwab and Bridle (1989), p. 315.

Rogers, A. E. E. 1991. "Very long baseline interferometry fringe detection thresholds for single baselines and arrays". In H. Hirabayashi, M. Inoue, and H. Kobayashi (Eds.), *Frontiers of VLBI.* Tokyo: Universal Academy Press, Inc., p. 341.

Rogers, A. E. E. 1993a. "Detection threshold for global fringe fitting". VLBA Scientific Memorandum 3, National Radio Astronomy Observatory.

Rogers, A. E. E. 1993b. "Weak source detection: Comparison of two methods". VLBA Scientific Memorandum 4, National Radio Astronomy Observatory.

Rogers, A. E. E., Cappallo, R. J., Hinteregger, H. F., Levine, J. I., Nesman, E. F., Webber, J. C., Whitney, A. R., Clark, T. A., Ma, C., Ryan, J., E., Corey B., C., Counselman C., Herring, T. A., Shapiro, I. I., Knight, C. A., Shaffer, D. B., Vandenberg, N. R., Lacasse, R., Mauzy, R., Rayhrer, B., Schupler, B. R., & Pigg, J. C. 1983. "Very-long-baseline radio interferometry: The Mark III system for geodesy, astrometry, and aperture synthesis". *Science* **219**, 51.

Rogers, A. E. E., Doeleman, S. S., & Moran, J. M. 1995. "Fringe detection methods for very long baseline arrays". *Astron. J.* **109**, 1391.

Rudnick, L., Zukowski, E., & Kronberg, P. P. 1983. "Measurement of unambiguous rotation measures of extragalactic sources". *Astron. Astrophys. Suppl.* **52**, 317.

Simon, R. S., Readhead, A. C. S., Moffet, A. T., Wilkinson, P. N., Booth, R., Allen, B., & Burke, B. F. 1990. "Images of four compact steep-spectrum quasars with a resolution of 20 milliarcseconds at 329.1 MHz". *Astrophys. J.* **354**, 140.

Thompson, A. R., Moran, J. M., & Swenson, G. W., Jr. 1986. *Interferometry and Synthesis in Radio Astronomy.* New York: Wiley-Interscience. First (1991) and second (1994) reprintings by Krieger Pub. Co., Malabar (Florida).

van Gorkom, J. H., Knapp, G. R., Ekers, R. D., Ekers, D. D., Laing, R. A., & Polk, K. S. 1989. "HI absorption in radio elliptical galaxies—evidence for infall". *Astron. J.* **97**, 708.

Walker, R. C. 1989. "Sensitivity". See Felli and Spencer (1989), p. 163.

Wardle, J. F. C., & Kronberg, P. P. 1974. "The linear polarization of quasi-stellar radio sources at 3.71 and 11.1 centimeters". *Astrophys. J.* **194**, 249.

Wilkinson, P. N., Tzioumis, A. K., Benson, J. M., Walker, R. C., Simon, R. S., & Kahn, F. D. 1991. "A disrupted radio jet inside the host galaxy of the quasar 3C 84". *Nature* **352**, 313.

Wrobel, J. M. 1994. "VLBA observational status summary". Technical report, National Radio Astronomy Observatory.

Wrobel, J. M., & Claussen, M. J. 1994. "Very long baseline interferometry at the VLA". Technical report, National Radio Astronomy Observatory.

Wrobel, J. M., & Simon, R. S. 1986. "92 Centimeter VLBI structure of the elliptical galaxy MCG 5-4-18". *Astrophys. J.* **309**, 593.